RESEARCH ARTICLE | *Control of Movement*

Separable systems for recovery of finger strength and control after stroke

Jing Xu,[1]* Naveed Ejaz,[2,3]* Benjamin Hertler,[4] Meret Branscheidt,[4,7] Mario Widmer,[4]
Andreia V. Faria,[5] Michelle D. Harran,[6] Juan C. Cortes,[6] Nathan Kim,[1] Pablo A. Celnik,[7]
Tomoko Kitago,[6] Andreas R. Luft,[4,8] John W. Krakauer,[1] and Jörn Diedrichsen[2,3]

[1]*Department of Neurology and Neurosciences, Johns Hopkins University, Baltimore, Maryland;* [2]*Institute of Cognitive Neuroscience, University College London, London, United Kingdom;* [3]*Brain Mind Institute, Western University, London, Ontario, Canada;* [4]*Division of Vascular Neurology and Rehabilitation, Department of Neurology, University Hospital and University of Zürich, Zürich, Switzerland;* [5]*Department of Radiology, Johns Hopkins University, Baltimore, Maryland;* [6]*Department of Neurology, Columbia University, New York, New York;* [7]*Department of Physical Medicine and Rehabilitation, Johns Hopkins University, Baltimore, Maryland; and* [8]*Cereneo Center for Neurology and Rehabilitation, Vitznau, Switzerland*

Xu J, Ejaz N, Hertler B, Branscheidt M, Widmer M, Faria AV, Harran MD, Cortes JC, Kim N, Celnik PA, Kitago T, Luft AR, Krakauer JW, Diedrichsen J. Separable systems for recovery of finger strength and control after stroke. *J Neurophysiol* 118: 1151–1163, 2017. First published May 31, 2017; doi:10.1152/jn.00123. 2017.—Impaired hand function after stroke is a major cause of long-term disability. We developed a novel paradigm that quantifies two critical aspects of hand function, strength, and independent control of fingers (individuation), and also removes any obligatory dependence between them. Hand recovery was tracked in 54 patients with hemiparesis over the first year after stroke. Most recovery of strength and individuation occurred within the first 3 mo. A novel time-invariant recovery function was identified: recovery of strength and individuation were tightly correlated up to a strength level of ~60% of estimated premorbid strength; beyond this threshold, strength improvement was not accompanied by further improvement in individuation. Any additional improvement in individuation was attributable instead to a second process that superimposed on the recovery function. We conclude that two separate systems are responsible for poststroke hand recovery: one contributes almost all of strength and some individuation; the other contributes additional individuation.

NEW & NOTEWORTHY We tracked recovery of the hand over a 1-yr period after stroke in a large cohort of patients, using a novel paradigm that enabled independent measurement of finger strength and control. Most recovery of strength and control occurs in the first 3 mo after stroke. We found that two separable systems are responsible for motor recovery of hand: one contributes strength and some dexterity, whereas a second contributes additional dexterity.

finger individuation; strength; stroke; motor recovery; plasticity

THE HUMAN HAND possesses a large repertoire of movements. Two critical aspects span its functional space: strength, as manifested in power grip, and control of individual finger movements, as in piano playing (Connolly and Elliott 1972; Napier 1956). The most common observation after stroke is that both are impaired (Kamper and Rymer 2001; Lang and

Schieber 2003). Weakness in both finger flexion and extension leads to difficulties in producing a strong grip and opening the hand (Colebatch and Gandevia 1989; Kamper et al. 2003). Loss of finger control manifests as inability either moving a single finger while keeping the others immobile or making complex hand gestures, both of which impair the ability to perform tasks such as typing or buttoning a shirt (Kamper and Rymer 2001; Lang and Schieber 2004; Li et al. 2003). When strength does recover after stroke, control often remains impaired, causing lasting disability (Heller et al. 1987; Sunderland et al. 1989). However, the relationship between strength and control after stroke remains poorly understood. Separating the effect of stroke on finger strength vs. control is a challenge given that most current clinical measurements cannot adequately separate weakness from deficits in control. In the current study we therefore sought to develop a new paradigm that could measure these two aspects of hand function separately and to investigate the relationship between strength and control over the time course of hand recovery after stroke. We were specifically interested in testing whether these two components recover in a lawful relationship with each other or whether they recover independently.

To isolate these two aspects of hand function, it is necessary to remove any obligatory relationship between them (Reinkensmeyer et al. 1992), i.e., derive a control measure that is independent of strength. Intuitively, a rock climber may have stronger fingers than a pianist but not necessarily superior control of individual fingers. Schieber (1991) devised an individuation task requiring participants to move individual fingers while attempting to keep the nonmoving ones stationary. Movements of the uninstructed fingers were used as a measure of loss of control. This paradigm, however, does not assess the relationship between forces that patients can generate and individuation ability. In the paradigm used in the present study, we first measured the maximum voluntary contraction force (MVF) that participants could produce with each finger. We then asked participants to produce isometric forces over four submaximal levels with each finger while trying to keep the uninstructed fingers immobile. Even healthy people show involuntary force production (enslaving) on the uninstructed

* J. Xu and N. Ejaz contributed equally to this work.
Address for reprint requests and other correspondence: J. Xu, Dept. of Neurology, School of Medicine, Johns Hopkins University, Pathology 2-210, 600 N. Wolfe St., Baltimore, MD 21287 (e-mail: jing.xu@jhmi.edu).

fingers, which increases with the required instructed finger force level (Li et al. 1998; Zatsiorsky et al. 2000). The slope of the function of uninstructed finger enslaving on instructed finger force thus provides a measure of individuation that is independent of strength.

Using this paradigm, we tracked the recovery of hand strength and finger individuation in patients over a 1-yr period after stroke. One possibility is that strength and control recover independently. For example, a patient may remain quite weak but have good recovery of individuation, or a patient may recover a significant amount of grip strength but fail to individuate the digits. Alternatively, recovery may be such that when strength recovers, so does individuation, because either they share a common neural substrate, or biological repair processes proceed at similar rates in separate neural substrates. Using fine-grained behavioral analysis, we show that the recovery of strength and individuation is mediated by two separable systems: one contributes mainly strength but also some individuation, whereas the other contributes additional individuation. Lesion analysis provided a clue as to what the anatomical basis for this separation might be.

MATERIALS AND METHODS

Participants

Fifty-four patients with first-time ischemic stroke and hemiparesis (34 men, 20 women; mean age 57.4 ± 14.9 yr) were recruited from three centers: The Johns Hopkins Hospital and Affiliates, Columbia University Medical Center, and The University Hospital of Zurich and Cereneo Center for Neurology and Rehabilitation. According to the Edinburgh Handedness Inventory (Oldfield 1971), 44 patients were right-handed and 10 were left-handed. All patients met the following inclusion criteria: *1*) first-ever clinical ischemic stroke with a positive DWI (diffusion-weighted imaging) lesion within the previous 2 wk, *2*) one-sided upper extremity weakness [Medical Research Council scale (MRC) <5], and *3*) ability to give informed consent and understand the tasks involved. We excluded patients with one or more of the following criteria: initial upper extremity Fugl-Meyer assessment (UE FMA) >63/66 (Fugl-Meyer et al. 1975), age under 21 yr, hemorrhagic stroke, space-occupying hemorrhagic transformation, bihemispheric stroke, traumatic brain injury, encephalopathy due to major nonstroke medical illness, global inattention, large visual field cut (greater than quadrantanopia), receptive aphasia (inability to follow 3-step commands), inability to give informed consent, major neurological or psychiatric illness that could confound performance/recovery, or a physical or other neurological condition that would interfere with arm, wrist, or hand function recovery. Due to the exclusion of aphasic patients, the sample had a bias toward right-sided infarcts (17 left-sided, 37 right-sided). The lesion distribution is shown in Fig. 6*A*. Of the 54 patients, 21 were on fluoxetine or other types of serotonin reuptake inhibitors (SRI) over the course of the study. For detailed patient characteristics, see Table 1.

We also recruited 14 age-matched healthy control participants (10 men, 4 women; mean age 64 ± 8.2 yr; all right-handed) at the three centers. There was no age difference between patient and control samples [2-sample *t*-test: $t(65) = 1.60$, $P = 0.11$], nor did the ratio of gender and handedness in the two groups differ (Fisher's exact test: $P = 0.11$ and 0.75, respectively). The healthy controls did not have any neurological disorder or physical deficit involving the upper limbs. All participants signed a written consent, and all procedures were approved by Institutional Research Board at each study center.

Assessment of Finger Maximum Voluntary Contraction and of Individuation

To achieve good characterization of hand function recovery, the study design required patient testing at the following five time points poststroke: within the first 2 wk (W1; 10 ± 4 days) and at 4–6 wk (W4; 37 ± 8 days), 12–14 wk (W12; 95 ± 10 days), 24–26 wk (W24; 187 ± 12 days), and 52–54 wk (W52; 370 ± 9 days). Healthy controls were tested at comparable intervals.

At each of the five visits, hand function was tested using an ergonomic device that measures isometric forces produced by each finger (Fig. 1*A*). The hand-shaped keyboard comprised 10 keys. Force transducers (FSG-15N1A, Honeywell; dynamic range 0–50 N) measured the downward flexion force exerted at each fingertip with a sampling rate of 200 Hz. The data were digitized using National Instrument USB-621x devices interfacing with the MATLAB (The MathWorks, Natick, MA) Data Acquisition Toolbox. Visual stimuli were presented on a computer monitor, run by custom software written in MATLAB environment using the Psychophysics Toolbox (Psychtoolbox; Brainard 1997).

Participants were seated in a comfortable chair, facing the computer monitor. Throughout the experiment, participants rested their two hands on the keyboards with each finger on top of a key, their wrists strapped and fixed on a wrist rest, with forearms extended and supported by foam arm rests. Ten vertical gray bars representing the 10 digits were shown at the top of the screen, and another 10 vertical bars below them instructed the amount of force to be exerted; the required force level for each finger per trial was indicated by the height of a green section within one of the vertical gray bars (Fig. 1*B*). Participants could monitor the force exerted by all 10 fingers in real time by the heights of 10 small white horizontal lines moving along the vertical force bars.

Two separate aspects of finger function were tested: maximal voluntary contraction force (MVF) and individuation. During each MVF trial, participants were asked to depress one finger at a time with maximum strength, and to maintain this force level for 2 s. The participants could press with the other fingers as much as they wanted as long as maximal force on the instructed finger was achieved. To signal the start, one force bar corresponding to the instructed finger turned green. MVF was measured twice per finger.

In each individuation trial, participants had to press only one finger at a sub-MVF force level while at the same time keeping other fingers immobile on the keys. Four target force levels were tested for each finger: 20%, 40%, 60%, and 80% of MVF; each level was repeated 4 times. On each trial, the participant was asked to bring the corresponding white line up to the force target line (black line in the middle of green region, representing the 25% upper and lower bounds of target force level; Fig. 1*B*) and to maintain the force level for 0.5 s. If no response passing the force threshold of 2.5 N was detected within 2 s, the trial was terminated.

Clinical Assessments

At each visit, all participants were also assessed with several clinical outcome measures. In this article we report data for the FMA and the Action Research Arm Test (ARAT; Lyle 1981). The UE FMA, a clinical measure of motor impairment (World Health Organization 2002), was graded by a trained assessor using the UE Fugl-Meyer (FM) scale, where a higher score connotes lower impairment (Fugl-Meyer et al. 1975). We summarized subscores for the entire upper extremity (FM-Arm; maximum 66) and hand (FM-Hand; maximum 14).

Data Analysis

Strength index. The 95th percentile of the force traces produced across all sampled force data points during the finger-depressing

Table 1. *Patient characteristics*

Patient	Age at Stroke, yr	Sex	Paretic Side	Initial FM-Arm	Initial MoCA	SRI
1	57	M	R	48	27	No
2	24	M	L	35	23	No
3	67	F	R	16	23	Fluoxetine
4	74	F	R	39	17	No
5	61	F	L	48	26	No
6	59	F	R	60	28	Sertraline
7	57	M	R	54	27	No
8	66	M	L	65	25	No
9	42	F	R	5	18	No
10	65	M	L	30	25	No
11	66	F	L	60	19	Fluoxetine
12	51	M	L	34	25	No
13	63	F	L	57	26	No
14	55	M	L	0	26	Fluoxetine
15	56	M	L	38	25	Fluoxetine
16	56	M	L	64	24	No
17	64	F	R	20	16	Trazodone
18	60	F	R	55	21	Fluoxetine
19	64	M	L	63	25	Fluoxetine
20	25	F	L	42	29	Fluoxetine
21	39	F	L	47	20	Fluoxetine
22	46	M	L	9	27	Fluoxetine
23	53	F	L	4	29	No
24	66	M	L	59	24	Escitalopram
25	71	M	L	4	26	No
26	52	M	L	53	24	No
27	46	M	R	4	21	Trazodone
28	46	M	L	49	30	No
29	71	M	L	6	24	No
30	47	M	R	57	10	No
31	45	M	L	8	27	No
32	55	F	L	19	25	Escitalopram
33	68	F	L	61	NaN	Escitalopram
34	65	M	L	32	28	No
35	51	F	L	63	26	Escitalopram
36	42	M	R	54	25	No
37	58	M	L	4	24	No
38	41	F	L	4	23	No
39	35	M	L	4	29	Escitalopram
40	68	M	L	52	27	Escitalopram
41	76	M	L	53	18	Sertraline
42	86	M	L	54	20	Escitalopram
43	48	M	L	16	25	No
44	74	M	R	5	25	No
45	80	F	R	9	24	No
46	64	F	L	58	19	No
47	22	M	R	63	27	No
48	88	F	R	55	28	No
49	22	M	R	63	27	No
50	87	F	R	50	28	No
51	84	M	R	30	26	Escitalopram
52	53	M	R	30	29	No
53	54	M	L	59	21	No
54	58	M	R	61	23	No

Data indicate patient age (years), sex (M, male; F, female), paretic side (L, left; R, right), initial Fugl-Meyer arm score (FM-Arm, maximum 66), initial Montreal Cognitive Assessment (MoCA, maximum 30), and serotonin reuptake inhibitor (SRI), if applicable. NaN, not a number (missing value).

period in each trial was calculated and then averaged across the two MVF trials to obtain a measure of MVF for each digit. If the force achieved on one of the two trials was below 60% of that produced on the other trial, only the larger force was taken as the MVF measure (6.5% of trials were excluded). The overall strength of the hand was then calculated by averaging across all five digits. To account for large intersubject variability in premorbid strength, all MVF values were normalized by MVF of the nonparetic hand at W52, estimated using a mixed-effects model (see below). This normalization provided a Strength Index, with a value close to 1 implying full recovery. For control participants, one hand was randomly assigned as the "nonpa-

retic" hand for normalization purposes. To account for possible laterality effects, the assignment followed the ratio of dominant to nondominant hands found in the patients (~10:4).

Individuation index. If individuation were perfect, a participant should be able to press the instructed finger without any force being exerted by the uninstructed fingers. For each time bin t (5 ms) in a single trial, the enslaved deviation of the force of each uninstructed finger ($F_{t,j}$) from baseline force (BF_j) was calculated, assessed at the beginning of the trial when a go cue was presented. This deviation was averaged over all bins (T) in the force trace from the go cue to the end of the trial:
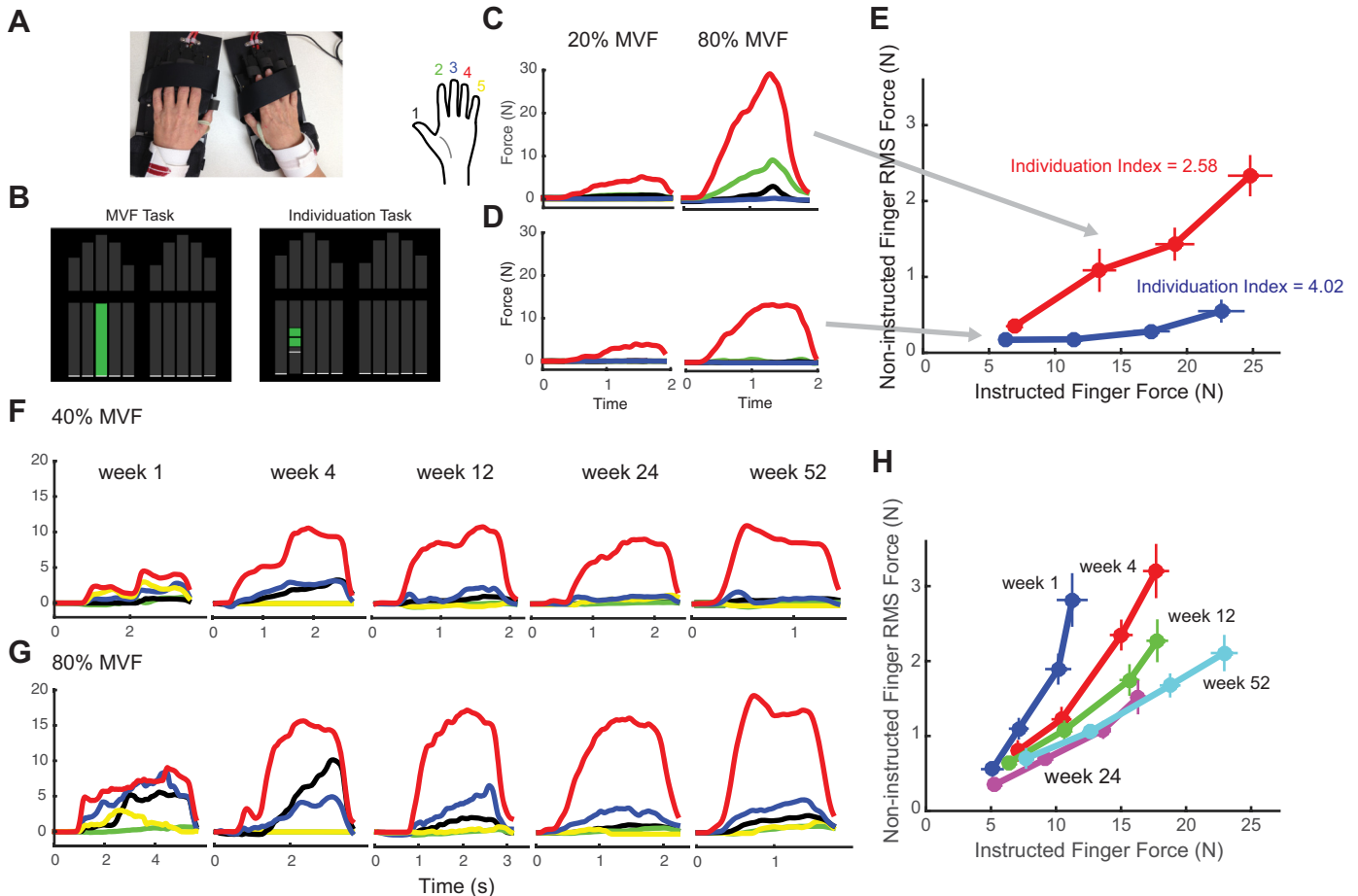
Fig. 1. Strength and individuation task. Fifty-four patients and 14 healthy controls were tested 5 times over a 1-yr period. *A*: ergonomic hand device. Force transducers beneath each key measured the force exerted by each finger in real time. The participant's fingers are securely placed on the keys using Velcro straps. *B*: computer screen showing the instructional stimulus, which indicates both which finger to press and how much force to produce (height of the green bar). In the MVF task, maximal force was required. MVF trials were performed twice on each finger. In the individuation task, 1 of 4 target force levels had to be reached. Target force levels were 20%, 40%, 60%, and 80% of MVF for each finger. Individuation trials were performed 4 times per force level per digit. *C* and *D*: example trials from 2 healthy control participants during the individuation task. Four trials are shown, one at 20% and one at 80% of MVF for the 2 participants. In this case the fourth finger (*inset*, red) was the instructed finger. Note the higher level of enslaving of the uninstructed fingers for higher instructed finger force level. *E*: mean deviation from baseline in the uninstructed fingers plotted against the force generated by the instructed finger for *C* and *D*. The Individuation Index is the −log (slope) of the regression line between instructed finger force and uninstructed mean deviation, measured as root mean square (RMS) force from baseline force produced by uninstructed fingers. *F* and *G*: example trials from 1 patient during the individuation task, two trials from each time point over the 1-yr period at 40% (*F*) and 80% MVF (*G*). The instructed finger for each trial was the same as those shown in control data (*C* and *D*). *H*: force-control trade-off function at each time point for the example patient, showing higher level of enslaving early after stroke and recovery of individuation ability over time.

$$meanDevP = \frac{1}{T}\sum_{t=0}^{T}\sqrt{\sum_{j=passive}(F_{t,j} - BF_j)^2}, \qquad (1)$$

where index j denotes the jth uninstructed finger. A higher mean deviation indicates more enslaving of the uninstructed finger.

For a measure of individuation ability, it is necessary to account for the relationship between force deviations of the uninstructed fingers and the force produced by the instructed finger. Consistent with previous reports (Li et al. 1998), we observed that enslaving of uninstructed fingers increases with higher instructed finger force (Fig. 1, *E* and *H*). The relationship between the two variables was close to linear. Thus a good measure of individuation reflects how much the mean deviation in uninstructed fingers increases for each Newton of force produced by the instructed finger. The ratio of these two variables can be reliably estimated by fitting a regression line without an intercept. To reduce the influence of outliers, we used robust regression (Holland and Welsch 1977). The slope of the regression line reflects individuation ability: a smaller slope corresponds to better individuation, with 0 being the best case, meaning that the unin-structed fingers are perfectly immobile at any instructed finger force

level. Because the regression slope is bounded by 0 (because mean deviation is positive), its distribution is positively skewed. To allow for the use of parametric statistics, the slope was log-transformed. The sign of this value was inverted so that higher values would correspond to better function. The negative log slope was calculated separately for each instructed finger and then averaged across fingers. The same normalization procedure as for the Strength Index was then applied to the averaged negative log slope to provide the final Individuation Index.

Reliability measures for strength and individuation. To determine the reliability of the Strength and Individuation Indexes, split-half reliabilities for both measures were calculated. For the Strength Index, we used one MVF trial per digit in each split. We then calculated the Strength Index (normalized) on each half of the data independently in the same way as for the full data set. The correlation between the two halves across all available sessions and patients was then used as a measure of split-half reliability.

For the Individuation Index, data from each finger were split such that two trials per force level were assigned to each split. The Individuation Index was then calculated separately for each split from

the slope of the regression line and normalized in the same way as Strength Index. We repeated the split multiple times, each time assigning trials at random and then averaging the split-half correlations from all splits for more reliable results.

Split-half correlation will underestimate reliability because the variability in each half will be higher than the variability when all the data are used (Guttman 1945). The estimate was therefore corrected using the formula

$$r_{full} = \frac{2r_p}{r_p + 1}, \quad (2)$$

where r_p is the correlation between the two splits.

Stability analysis. To assess whether the relative deficits in strength and individuation remained stable across different testing time points or whether there was meaningful biological change, we calculated the correlation of each measure across neighboring testing time points. One caution when interpreting these correlations is that the correlation between two repeated measures will always be smaller than 1 even if the underlying factor did not change, because both measures contain some measurement noise. To account for this effect, we used the reliability (r_{full}) of the measure at each time point to compute a noise ceiling, which indicates how much two repeated noisy measurements should correlate with each other if the underlying variable were perfectly stable:

$$r_{noise\ ceiling} = \sqrt{r1_{full} * r2_{full}}. \quad (3)$$

Statistical analysis and handling of missing data. Data analysis was performed using custom-written MATLAB and R (R Core Team 2012) routines. The analysis focused on the Strength and Individuation Indexes, but was also performed on standard clinical assessments, FMA and ARAT.

The requirement for five poststroke time points was ambitious, with the consequence of some missing sessions. A total of 21 patients completed all 5 time points; on average, each patient completed 3.6 sessions (total number of patients at each time point is 39, 39, 40, 39, and 34 for W1–52, respectively); thus a total of 75% of the possible sessions was acquired. Missing sessions were treated as data missing at random. To optimally use all the measured data, we employed linear mixed-effect models. The models specify joint distributions for observed and missing observations. Parameters of these distributions can thus be estimated by maximizing the likelihood of the data under the model. There are several advantages to this approach. First, all the available data can be used, and there is no need to exclude any data. Second, it avoids the statistical pitfalls inherent in "filling in" missing observations with point estimates. Linear mixed-effect models implemented in the *lme4* package in R (Bates et al. 2015) were used to test changes in these measures over time. Participant was taken as a random factor. Time point (5 time points from W1 to W52) and hand condition (paretic, nonparetic, and control) were considered fixed factors. The model was applied to control and patient data separately. Mixed-effect model estimation for group summary statistics was implemented in MATLAB using the restricted maximum likelihood method (Laird and Ware 1982).

Modeling the time-invariant function. To test the hypothesis that there is a time-invariant relationship between strength and individuation, a two-segment piecewise linear function was fitted. This function had four free parameters: the intercept, the location of the inflection point, and the slope on each side of the inflection point. Let x be the predictor with two segments separated by a constant breakpoint c, $x_1 \leq c$ and $x_2 \geq c$. The linear functions for each segment are

$$\begin{aligned} y_{1i} &= b_{10} + b_{11}x_{1i} + e_{1i} \\ y_{2i} &= b_{20} + b_{21}x_{2i} + e_{2i} \end{aligned}. \quad (4)$$

The two pieces can be joined at the breakpoint constant c by setting $y_{1i} = y_{2i}$, yielding

$$\begin{aligned} b_{20} &= b_{10} + (b_{11} - b_{21})c \\ y_{2i} &= b_{10} + (b_{11} - b_{21})c + b_{21}x_{2i} + e_{2i} \end{aligned}. \quad (5)$$

Putting the two pieces together, we have the full model

$$y_i = a + b_1 x_i \cdot I(x_i \leq c) + [(b_1 - b_2)c + b_2 x_i] \cdot I(x_i \geq c) + e_i, \quad (6)$$

where $I(\cdot)$ is an indicator variable, coded as 1 or 0 to indicate the condition satisfied.

The maximum-likelihood (least squares) estimates of these parameters were obtained by using the nonlinear optimization routine fminsearch in MATLAB. This time-invariant model with fixed parameters across all time points was then compared with a more complex model that allowed free parameters for each time point, using leave-one-out cross-validation (Picard and Cook 1984) to assess whether this function changed systematically over time or whether it was time invariant. Cross-validation provides an unbiased estimate of a model's ability to predict new data and automatically penalizes models that are too complex.

Lesion Imaging and Quantification

Imaging acquisition and lesion distribution. Images were acquired following the same testing schedule as behavior assessment, using a 3T MRI Phillips scanner, and consisted of two diffusion tensor imaging (DTI) data sets (TR/TE = 6,600/70 ms, echo-planar imaging, 32 gradient directions, $b = 700$ s/mm^2) and a magnetization-prepared rapid-acquisition gradient echo (MPRAGE) T1-WI sequence (TR/TE = 8/3.8 ms). Field of view, matrix, number of slices, and slice thickness were 212×212 mm, 96×96 (zero-filled to 256×256), 60, and 2.2 mm, respectively, for DTI and 256×256 mm, 256×256, 170, and 1.2 mm, respectively, for T1-WI. The DTI were processed using DtiStudio (www.mristudio.org), and the mean diffusion-weighted image (DWI) was calculated.

To define the boundary(ies) of the acute stroke lesion(s) for each participant, a threshold of >30% intensity increase from the unaffected area in the first-time point DWI extracted from DTI images (Leigh et al. 2013) was first applied. A neuroradiologist (AVF), blind to the patients' clinical information, then manually modified the boundary to avoid false-positive and false-negative areas on the RoiEditor software (www.mristudio.org). Following the standard in the field, the definitions were double checked by a second rater (MB). The averaged lesion distribution map across all patients in the current study is shown in Fig. 5A. For the seven patients who had no DTI in the acute phase, lesion definition was performed on the clinical DWI, which has lower resolution (1×1 mm in plane, thickness 4–6 mm). Analysis of white matter regions of interest (ROIs), including the corticospinal tract (CST), was not performed in these seven patients.

Region of interest definition and lesion quantification. The focus was on two ROIs: *1*) the cortical gray matter of the hand area in the motor cortex and *2*) the entire CST superior to the pyramids, identified by probabilistic maps derived from tract tracing methods (see below). Percent volume affected in these regions was computed as a ratio of the number of voxels affected by the lesion divided by the total number of voxels in the entire ROI. This measure was correlated with our main outcome measures, the Strength and Individuation Indexes.

To define the CST, each image and respective lesion was first mapped to a single-subject adult template, the JHU-MNI atlas (Mori et al. 2008; Oishi et al. 2008), using affine transformation followed by dual-channel (both b0 and FA maps) large deformation diffeomorphic metric mapping (LDDMM) (Ceritoglu et al. 2009). This template has already been segmented into more than 200 ROIs and contains probabilistic maps of multiple tracts, including the CST (Mori et al. 2005; Oishi et al. 2010; Zhang et al. 2010). To ensure accurate mapping in the lesioned areas, we first used "artificial" images in which the stroke area was masked out and substituted by the normal images from the contralateral hemisphere. This helped minimize

inaccuracies caused by focal changes in intensity due to the stroke. In addition, also to avoid inaccuracy caused by lesion, we directly applied the probabilistic map of the CST to each patient's image. The original probabilistic map CST was defined on the basis of data from 20 healthy participants in a previous study (Zhang et al. 2010), using an automated fiber assignment by continuous tractography (FACT) method (Wakana et al. 2007; Zhang et al. 2008). Specifically, the initial seeds were placed in the middle portion of cerebral peduncle and traced back to the precentral (primary motor) cortex. Multiple reference ROIs were then placed in regions along the tracts, including the pyramids, to which "NOT," "AND," "CUT," and "OR" logic operations were applied, to ensure that the delineation was as consistent as possible with existing anatomical knowledge of the CST. Lateral motor cortices were not included because of mixing of fibers with different orientations within each pixel. The particular sequence of ROIs and logic operations used to isolate the CST reflects a trade-off between sensitivity and reliability, and has been shown to have a high level of intra- and inter-rater reproducibility (Wakana et al. 2007). The white matter tracts were identified with a fractional anisotropy threshold of 0.2. The probabilistic map was then "back-warped" to each patient's individual space by a series of LDDMM mapping.

A different approach was used to define an ROI that would encompass the hand area of the primary motor cortex. The hand ROI was defined on the average reconstruction of the cortical surface available in the FreeSurfer software (Dale et al. 1999), selecting Brodmann area (BA) 4 based on cytoarchitectonic maps (Fischl et al. 2008). To restrict the ROI to the area of motor cortex involved in the control of the upper limb, we only included the area 2.5 cm dorsal and ventral to the hand knob (Yousry et al. 1997). The defined ROI was then morphed into MNI space using the surfaces of the age-matched controls. These ROIs were then brought to the JHU-MNI atlas (in which each subject's image and respective stroke area were already mapped, as mentioned above) using T1-based LDDMM to construct a probabilistic map of the hand area. The probabilistic map was threshold of 70% to calculate percent volume affected.

RESULTS

In a large-scale longitudinal study, we tracked recovery of two behavioral components of hand function: strength and finger control, using a novel paradigm that measures them independently. A total of 54 patients with acute stroke and 14 healthy controls were tested 5 times over a 1-yr period. Data in the final analysis comprised a total of 251 sessions tested in 53 patients (1 patient only completed 2 blocks of the task and was thus removed from further analysis) and 14 controls. Forty-one patients and 12 controls completed ≥3 sessions (see details in MATERIALS AND METHODS).

Strength and Individuation Indexes Were Reliable

At each of the five visits, hand function was tested using an ergonomic device that measures isometric forces produced by each finger (Fig. 1A). Two separate aspects of finger function were tested: strength (MVF) and individuation (Fig. 1B).

Finger strength was assessed by measuring MVF for each finger separately and then averaged across all fingers for each hand. MVF for healthy controls had an average value of 20.35 N (SD 8.56) for the dominant hand and 22.76 N (SD 6.89) for the nondominant hand. The normalized Strength Index (see MATERIALS AND METHODS) for the controls' dominant hand was 1.00 (SD = 0.19), and that for the nondominant hand was 1.17 (SD 0.25). For patients, the mean for the nonparetic hand was 0.93 (SD 0.20), and that for the paretic hand was 0.59 (SD

0.38). For the paretic hand, Strength Indexes did not correlate with age ($r = 0.04$, $P = 0.75$) and were not affected by sex [$t(51) = 0.98$, $P = 0.33$] or handedness [$t(51) = 0.10$, $P = 0.92$].

To assess individuation, we measured the amount of involuntary force changes on the uninstructed fingers (enslaving; Zatsiorsky et al. 2000) for different levels of force production with the instructed fingers. The amount of enslaving systematically increased at higher force levels (Fig. 1, C–H). Loss of control at increasing force levels has been shown for angular position of the fingers (Li et al. 1998) and reaching radius of the arm after stroke (Sukal et al. 2007). To control for this relationship, we characterized the Individuation Index as the slope of the function between instructed finger force and uninstructed enslaving (see MATERIALS AND METHODS). Lower values of the Individuation Index indicate more impaired individuation. Healthy, age-matched controls showed, on average, a normalized Individuation Index of 1.00 (SD 0.18). This refers to a slope of 0.087 (SD 0.046), meaning that for a finger press of 10 N, the mean deviation of the uninstructed fingers was 0.69 N. As was the case for strength, Individuation Indexes in the paretic hand were not correlated with age ($r = 0.16$, $P = 0.26$) and were not affected by sex [$t(51) = 0.17$, $P = 0.86$] or handedness [$t(51) = 0.34$, $P = 0.74$].

When a new instrument is being introduced, it is important to first establish its reliability, i.e., the accuracy with which true intersubject differences and intrasubject changes can be determined. We therefore split the data for each session in half, calculated Strength and Individuation Indexes on these two independent data sets, and correlated the resultant scores across patients and sessions (see MATERIALS AND METHODS). The adjusted split-half reliability across all patients and weeks for the Strength Index was $r_{full} = 0.99$ and 0.94 for the paretic and nonparetic hands, respectively, and $r_{full} = 0.89$ for controls, which indicates good reliability. The adjusted split-half reliability of the Individuation Index of all patients was $r_{full} = 0.99$ and 0.93 for the paretic and nonparetic hands, respectively, and $r_{full} = 0.97$ for controls.

Consistent with our effort to construct an individuation measure that is independent of strength, the overall correlation between individuation and strength was very low for controls ($r = -0.19$, $P = 0.51$).

Standard Clinical Measures Do Not Adequately Distinguish Between Strength and Individuation

We then compared the Strength and Individuation Indexes with existing clinical measures: the Fugl-Meyer scale (FM; a measure of impairment) and the action reach arm test (ARAT; a measure of activity). Table 2 shows the correlations for all four measures obtained from the paretic hand across all time points. Overall, all correlations were high (maximum $P = 1.21 \times 10^{-26}$), indicating that all the measures could detect severity of the hand function deficit. The correlation in the patients between the two clinical measures was 0.91, whereas the correlation between the Strength and Individuation Indexes was 0.73, a significant difference [$z = 5.62$, $P = 2.0 \times 10^{-8}$, using Fisher's z-test (Fisher 1921) with $n = 180$, the total no. of sessions for which both behavioral (Strength and Individuation Indexes) and clinical data (FM and ARAT) were

Table 2. *Correlation between Strength Index, Individuation Index, FM-Arm, and ARAT*

	Strength Index	Individuation Index	FM-Arm	ARAT
Strength Index		0.73	0.76	0.74
Individuation Index			0.68	0.72
FM-Arm				0.91

Data show the correlations between the Strength Index, Individuation Index, Fugl-Meyer arm score (FM-Arm, maximum 66), and Action Reach Arm Test (ARAT, maximum 57). All four measures were highly correlated; however, the Strength and Individuation Indexes showed a weaker correlation compared with that between the FM-Arm and ARAT.

available]. Given comparable reliabilities for all measures, this difference is unlikely to result from measurement noise; rather, it suggests that our Strength and Individuation Indexes better isolate strength and control than the clinical measures.

Recovery of Strength and Individuation Occurred Mainly in the First Three Months After Stroke

We first examined the time courses of recovery for strength and individuation in the paretic hand. If the two observed variables change in parallel, their recovery may or may not be mediated by the same underlying process. A difference in the time courses, however, would provide a strong hint of separate recovery processes for strength and individuation.

For both measures, most of the recovery appeared to occur within the first 12 wk after stroke (Fig. 2, *A* and *B*). A mixed model with a fixed effect of week and a random effect of subject was built to evaluate this statistically. An effect of week was tested with a likelihood ratio test against the null model with the random effect only. Results indicate that both Strength and Individuation Indexes significantly changed over time (strength: $\chi^2 = 47.65$, $P = 5.10 \times 10^{-12}$; individuation: $\chi^2 = 18.58$, $P = 1.63 \times 10^{-5}$). Paired *t*-tests between adjacent time points showed significant improvement (after Bonferroni correction) of the Strength Index up to W12, whereas the Individuation Index only showed a significant improvement between W4 and W12 (see detailed statistics in Fig. 2, *A* and *B*). A similar recovery curve was found for the standard clinical measures of motor function (detailed statistics in Fig. 3).

To directly compare the time courses between the two indexes at the early stage of recovery, we *z*-normalized scores of the two variables and then investigated the change in the scores for the time intervals W1–W4 vs. W4–W12 (Fig. 2*C*). This analysis suggests that strength may recover mostly in the first 4 wk, whereas individuation recovery may occur equally in both time periods. Repeated-measures ANOVA over *z*-normalized scores for Strength and Individuation Indexes during the two time intervals yielded a significant interaction [$F(1,25) = 6.82$, $P = 0.015$; Fig. 2*C*]. Thus, despite overall similarity, there was a significant difference in the time courses of recovery of strength and individuation, with strength showing faster early recovery.

That most improvement in both strength and individuation occurred over the first 12 wk can be observed not only in the mean recovery curve but also in the variability of interindividual differences between adjacent testing time points (Fig. 2*D*). The correlation between W1 and W4 across individuals
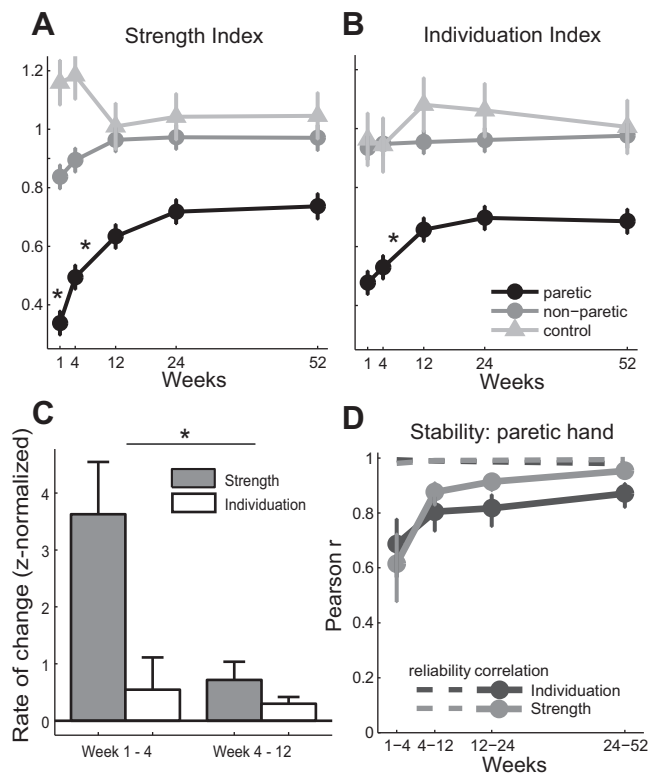

Fig. 2. Temporal profiles of recovery for strength and individuation. *A* and *B*: group recovery curves for the Strength and Individuation Indexes for patients and controls. Asterisks indicate significant week-to-week changes for the paretic hand [Bonferroni corrected *P* values for each segment of Strength Index: $P(W1–W4) = 0.0045$, $P(W4–W12) = 0.0082$, $P(W12–W24) = 0.068$, and $P(W24–W52) = 0.87$; Individuation Index: $P(W1–W4) = 0.81$, $P(W4–W12) = 0.0024$, $P(W12–W24) = 1.92$, and $P(W24–W52) = 2.91$]. *C*: rate of change (i.e., change per week) in *z*-normalized Strength and Individuation Indexes during the first 2 intervals (W1 to W4 and W4 to W12). The 2 intervals show a significant interaction between strength and individuation, indicating faster initial improvement of strength. *D*: week-to-week correlations between adjacent time points for the Strength and Individuation Indexes. Dashed lines are the noise ceilings based on the within-session split-half reliabilities (sample size $N = 53$ patients, 14 controls, with a total of 251 completed sessions).

for the Individuation Index was significantly lower than it was for subsequent time points (W1–W4 vs. W24–W52: $z = -4.23$, $P = 2.3 \times 10^{-5}$), and this difference for Strength Index was marginally significant [$z = -1.83$, $P = 0.067$, using
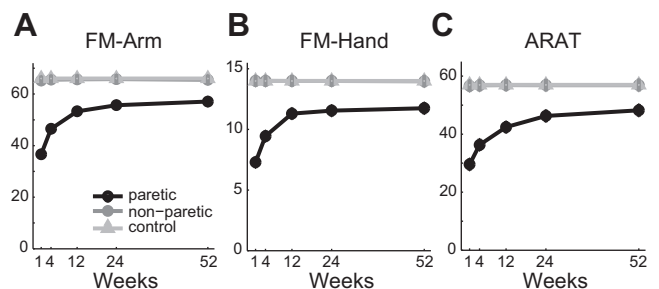

Fig. 3. Temporal recovery profiles for clinical measures: Fugl-Meyer for the arm (*A*; FM-Arm) and hand (*B*; FM-Hand) and the ARAT (*C*). All measures showed significant change over time for the paretic hand. FM-Arm: $\chi^2 = 37.73$, $P = 8.13 \times 10^{-10}$; FM-Hand: $\chi^2 = 29.03$, $P = 7.14 \times 10^{-8}$; ARAT: $\chi^2 = 36.33$, $P = 1.67 \times 10^{-9}$ (sample size $N = 53$ patients, 14 controls, with a total of 238 and 235 completed sessions for FM and ARAT, respectively).

Fisher's z-test (Fisher 1921) with $n = 28$ and 33]. Thus the relative position of the patients on the mean recovery curve changed more during the first 4 wk than during the second 6 mo. This correlation difference cannot be attributed to measurement noise, because both measures had high reliabilities at all time points (Fig. 2D, dashed lines). Instead, the lack of stability of these measures during early recovery is indicative of meaningful biological change accelerating some patients' recovery, but not others'.

Consistent with previous findings (Noskin et al. 2008), the nonparetic hand also showed mild impairment in the first month after stroke. A likelihood ratio test of the mixed-effect model showed a significant effect of week for strength ($\chi^2 = 7.86$, $P = 0.0051$) and a more subtle effect for individuation ($\chi^2 = 4.12$, $P = 0.042$; Fig. 2, A and B). This increase in performance is unlikely to be related to a general practice effect, because the Strength Index in healthy controls decreased slightly over time ($\chi^2 = 4.54$, $P = 0.033$), perhaps due to reduced effort, whereas the Individuation Index for healthy controls was maintained at a similar level over the whole year ($\chi^2 = 0.33$, $P = 0.56$). Thus our results confirmed the previous finding that stroke appears to be associated with a mild ipsilateral deficit in hand function (Noskin et al. 2008).

In summary, most recovery of both strength and individuation occurred in the first 3 mo after stroke, with stabilization of recovery around 3–6 mo. The data also suggest a slight difference in the time courses, with strength recovering faster than individuation in the first month.

Evidence for a Time-Invariant Relationship Between Strength and Control

To examine the relationship between finger strength and control, we undertook a closer examination of how the two variables relate to each other by plotting one against the other at each testing time point (Fig. 4A). Interestingly, the resultant function has a distinct curvilinear shape that is preserved across weeks. At lower strength levels, there is a clear correlation between strength and individuation, whereas once strength recovers to above ~60% of normal levels, the two variables become uncoupled (Fig. 4B). Recovery is captured by a patient moving from the *bottom left* corner to the *top right* corner of this function.

To formally test that the function's curvilinear shape is indeed time invariant, i.e., it remains the same at all poststroke time points, we first found a function to describe the strength-individuation relationship. We used data from all time points and evaluated the goodness of fit of a piecewise function with two linear segments connected at an inflection point, using leave-one-out cross-validation (see MATERIALS AND METHODS). Cross-validation automatically penalizes models that are too complex. This functional form gave us good prediction of the data (cross-validated $R^2 = 0.53$; Fig. 4B). We also explored first- to fourth-order polynomial functions. All four models resulted in a worse prediction than the piecewise linear function (cross-validated $R^2 < 0.49$). We then tested whether the function shape is the same across weeks. With the use of leave-one-out cross-validation, the time-invariant model with fixed parameters across all weeks was compared against a model allowing the parameters to change for each week (time-varying model).

The cross-validated R^2 for the time-varying two-segment piecewise linear function was 0.45, a worse prediction than the time-invariant model.

These results suggest that there is indeed a time-invariant recovery relationship between strength and individuation after stroke: up to a certain level of strength (60.7% of nonparetic hand), Strength and Individuation Indexes are strongly correlated ($r = 0.74$, $P = 6.61 \times 10^{-18}$); after strength exceeds this threshold, the two variables are no longer correlated ($r = -0.17$, $P = 0.11$; Fig. 4B). This lack of correlation cannot be attributed to a ceiling effect for the Individuation Index, because even above this level, the intersubject variances were still higher than the intrasubject variances in both patients and controls, which attests to the high reliability of the Individuation Index. This indicates that our measure has enough dynamic range and sensitivity to detect interindividual differences even in the healthy population.

Overall, our results suggest that recovery can be captured as traversal along a time-invariant function relating strength and individuation. Differences in recovery arise because patients vary substantially in the distance they move along this function: some patients with initial severe impairment made a good recovery, moving past the inflection point of 60.7% strength (exemplified by the yellow circle in Fig. 4A). Other severely impaired patients failed to reach the inflection point (red circle in Fig. 4A) (Supplementary Video S1; supplemental material for this article is available online at the *Journal of Neurophysiology* website). Finally, some mildly impaired patients started off beyond the inflection point and showed a good range of individuation recovery.

A Second Process Contributed Additional Recovery of Finger Individuation

The fact that recovery of both strength and individuation could be captured by a single time-invariant function that relates them is compatible with the hypothesis of a single underlying process that drives recovery of both aspects of hand function. It is possible, however, that an additional process injects further recovery, which determines a patient's position relative to the mean recovery function. If such a process exists, a given patient should occupy a consistent position above or below the mean recovery function across time points. To test this hypothesis, we investigated the residuals of the Individuation Index for each patient at each time point after subtracting the mean two-segment piecewise linear recovery function. If the variability around this mean function were purely due to noise, we should observe no consistent week-by-week correlation between residuals for each patient. Alternatively, if the residuals were to be correlated across weeks, it would indicate that some patients were consistently better at individuation than would be predicted by the function, and others were consistently worse, suggesting an additional factor mediating individuation recovery (Fig. 5; vertical arrows).

Correlations of residuals from adjacent time points across patients were initially quite low. However, from W4 onward, most patients' distances from the mean function remained stable (Fig. 4, C and D). This consistent structure in residuals provides evidence for an extra factor contributing to the recovery of individuation. The high correlation of residuals at later time points
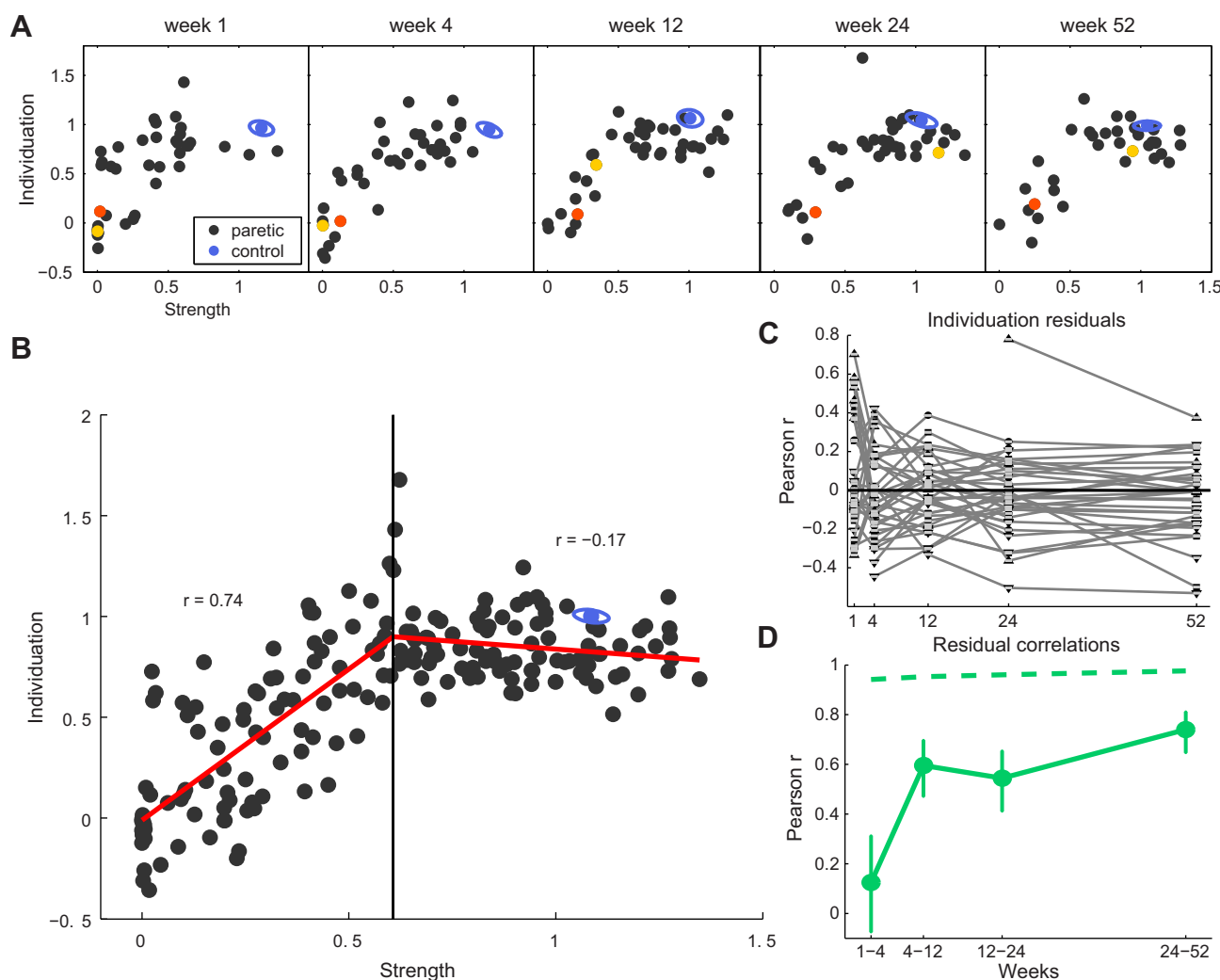
Fig. 4. Time-invariant impairment function relating strength and control. *A*: scatter plots for Individuation vs. Strength Indexes at each time point. Each black circle is one patient's data; blue circles and ellipse indicate the mean and SE for controls at the time point. Two patients' data are highlighted: one with good recovery (yellow circle) and one with poor recovery (red circle). The total number of patients at each time point is 39, 39, 40, 39, and 34 for W1–W52, respectively. *B*: scatter plot with data from all time points superimposed with the best-fitting two-segment piecewise linear function with one inflection point at Strength Index = 0.607. *C*: residuals from each week, with the mean impairment function (red line in *B*) subtracted. The tendency of the residuals to stay above or below the typical Strength-Individuation relationship indicates that there are stable factors that determine individuation recovery over and above strength recovery. *D*: correlations of residuals from *C* across adjacent time points increased over time [Bonferroni-corrected P(W1–W4) = 2.12, P(W4–W12) = 0.00064, P(W12–W24) = 0.0024, and P(W24–W52) = 3.39×10^{-6}]. Dashed line is the noise ceiling based on the within-session split-half reliabilities (sample size N = 53 patients, 14 controls, with a total of 251 completed sessions).

could not be attributed to premorbid interindividual differences, because both Strength and Individuation Indexes were normalized to the nonparetic hand. The low week-by-week correlations between early time points argue that the later correlations do not simply reflect sparing of a particular neural system after stroke. If this had been true, correlation between the individuation residuals should have remained constant across all time points. Furthermore, the lower early correlation cannot be attributed to measurement noise, because reliabilities for the early measurement points were high (Fig. 4*D*). Rather, the initially low but then increasing correlation indicates an additional recovery process operating above the lower bound of the strength-individuation function (Fig. 5). This process is mostly active in the first 3 mo after stroke and determines how well individuation recovers above that expected from the time-invariant recovery function.

Lesions Involving the Hand Area of Motor Cortex and the Corticospinal Tract Correlated More with Individuation Than with Strength

To investigate the underlying neural substrates of recovery processes, we correlated the location and size of the lesion with the Strength and Individuation Indexes. On the basis of classic nonhuman primate studies (Lawrence and Kuypers 1968a, 1968b), we predicted that individuation would integrally depend on the corticospinal tract (CST), whereas strength may have contributions from other tracts, such as the reticulospinal tract (RST). Whereas cells originating from the RST also receive cortical input from the precentral gyrus and are intermingled with the CST to some degree, cortical projections to the reticular formation have a more widespread bilateral origin from other premotor areas (Keizer and Kuypers 1989), whereas direct corticospinal projections to ventral horn motor neurons
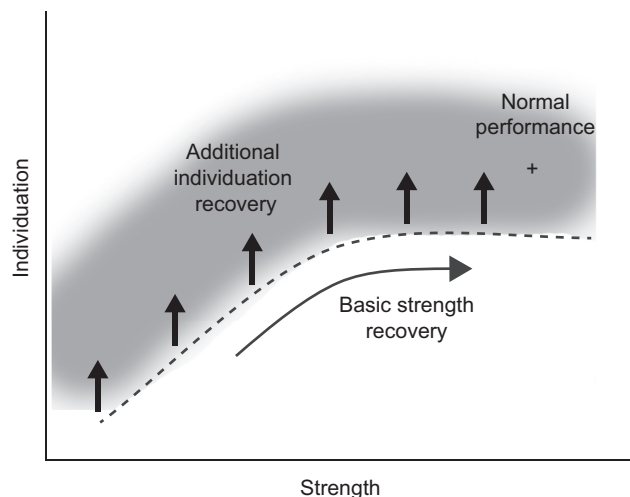
Fig. 5. Schematic diagram of the hypothesis for two recovery systems. The first system (basic strength recovery) underlies strength recovery and a restricted amount of individuation recovery. This system therefore defines the lower bound (dashed line) of the space occupied by recovering patients (gray shading). A second system (additional individuation recovery; vertical arrows) adds further individuation abilities on top of basic strength recovery.

because the Strength and Individuation Indexes had comparable reliabilities. Furthermore, percent lesion involvement also significantly correlated with the Individuation Index, after the average Strength-Individuation relationship was accounted for ($P < 0.05$ for correlations after W24 for cortical hand area and after W12 for CST). Indeed, at W52, correlations with the Individuation Index residuals were as high as with the Individuation Indexes themselves ($r = 0.61$ vs. $r = 0.57$ for the cortical hand area, $r = 0.51$ vs. $r = 0.54$ for the CST). Together, these results suggest that individuation recovery is most heavily determined by sparing in the hand area of the primary motor cortex and of CST projections, whereas strength recovery may also depend on other spared descending pathways.

DISCUSSION

We tested patients at five time points over a 1-yr period after stroke, using a novel paradigm that separately measures maximum voluntary contraction force (MVF; a measure of strength) and finger individuation ability (a measure of control), and crucially controls for any obligatory dependency between these two measures. This approach allowed us to determine how recovery of strength and control interrelate. Our main question was to ask whether strength and control shared the same recovery mechanisms, after the two variables had been experimentally uncoupled. If they are truly dissociable, then hypothetically patients could show perfect control of individual fingers, even with significant weakness (except for complete hemiplegia, in which case no individuation measure would be obtainable). We showed that involuntary movements in uninstructed fingers (enslaving) increased with the level of force production of the instructed finger. This phenomenon is analogous to what Sukal et al. (2007) have described for the paretic arm: loss of control as indicated by a decrease in the arm's reaching workspace as the force requirement to resist gravity increases. In the present study we used the ratio of enslaved and instructed finger forces as an Individuation Index, thereby isolating the control component and factoring out its dependence on force production. We show that this approach

primarily arise from the anterior bank of the precentral gyrus/central sulcus, i.e., "new M1" (Rathelot and Strick 2009; Witham et al. 2016). We therefore predicted that the extent of damage to the hand area of the primary motor cortex, and to the white matter ROI that characterizes the most likely course of the CST (see MATERIALS AND METHODS), would correlate more with individuation and less with strength. Furthermore, lesions in these areas should correlate with individuation recovery over and above the level expected from the mean recovery function.
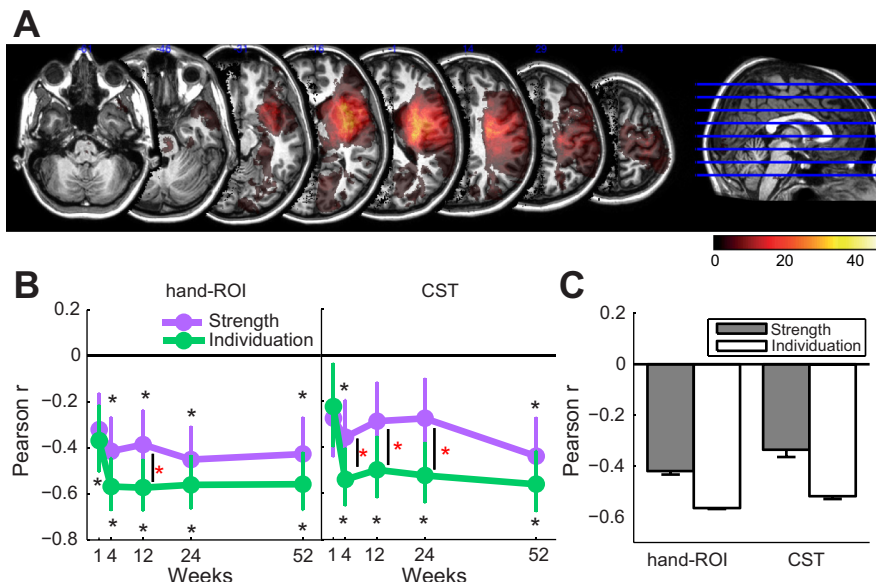
As hypothesized, the extent of involvement by the lesion of the cortical hand area correlated significantly with the Individuation Index at all time points. For the CST, all correlations were significant after W1 (Fig. 6, *B* and *C*). Although both lesion measures also correlated with the Strength Index, these correlations were weaker [repeated-measures ANOVA showed a significant main effect for behavioral measure: $F(1,3) = 146$, $P = 0.001$]. This difference was not due to measurement noise,

Fig. 6. Lesion distribution and correlation with behavior. *A*: averaged lesion distribution mapped to JHU-MNI space (see MATERIALS AND METHODS), with lesion flipped to one hemisphere. Color bar indicates patient count. *B*: correlation of behavior measures (Strength and Individuation Indexes) at each time point with the percentage of damaged cortical gray matter within the M1 hand area ROI and the corticospinal tract (CST). Black asterisks indicate significant correlations (tested against 0), and red asterisks indicate a significant difference ($P < 0.005$) between the correlation for strength and individuation for each week. *C*: mean of week-by-week correlations between the two behavior measures and percent lesion volume measures for the cortical gray matter hand area and CST ROIs (sample size $N = 53$, with 251 completed sessions).

provides a sensitive measure of finger control independent of the level of force deficit.

Our paradigm quantifies two critical dimensions of hand function, because we argue that real-life actions such as precision grip require a weighted combination of strength and precision control of individual fingers (Xu et al. 2015). There are of course limitations to this approach. Other dimensions, such as the use of tactile information from the fingertips, which are likely to be important for fine object manipulation, are not assessed in our task. Furthermore, we assess individuation capability in a medium-to-high force range (>20% MVF), whereas many fine motor actions demand lower levels of force. Note, however, that 20% MVF for many patients corresponded to 5–10% MVF for healthy controls in terms of absolute force and therefore falls into the range of forces needed for everyday fine-finger control actions. Overall, we think that our Strength and Individuation Indexes capture two fundamental aspects of hand function.

We first examined the time courses of recovery for strength and individuation. Consistent with what has been described with traditional clinical scales (Duncan et al. 1992; Jørgensen et al. 1995; Krakauer et al. 2012), both measures showed that most recovery occurred within the first 3 mo after stroke. This similarity between the time courses, however, does not necessarily imply that recovery of strength and individuation is dependent on a single underlying neural substrate or mechanism. It remains possible that recovery of these two components occurs in parallel because of commonalities in basic tissue repair mechanisms postischemia, but they are nevertheless independent modules. Indeed, we found a small but robust difference in the time course of recovery of strength compared with control: finger strength showed a faster rate of change compared with individuation over the first month.

Closer examination of the two variables revealed a time-invariant nonlinear relationship between strength and individuation in the paretic hand. This function has two distinct parts: individuation and strength were highly correlated below a strength threshold of ~60% of the nonparetic side; beyond this point, they were uncorrelated.

Recovery of hand function could be characterized as movement along the time-invariant function (it had the same shape across all time points): patients with good recovery traveled further along the function, whereas patients with poor recovery remained in the first segment. The existence of the recovery function suggests that a single system mediates recovery of both strength and individuation. This system can generate strength but has only limited individuation capacity; beyond this threshold, there can be further increases in strength but no accompanying improvements in individuation. It is important to note that the correlation at lower levels of strength recovery (<60%) does not represent a causal relationship between strength and individuation, because by definition the Individuation Index is corrected for strength. What this correlation at lower strength level is capturing instead is a shared underlying recovery process, not an obligatory strength-control relationship. The lack of a causal relationship is also apparent in the fact that some patients had a higher Individuation Index at relatively low levels of strength (<60%), whereas others regained full strength but were still impaired with individuation (Fig. 4B).

Our analysis also revealed clear evidence for a second system that contributes to recovery of individuation. There was systematic structure in the residuals around the mean recovery function: patients at the chronic stages differed consistently in the amount of individuation recovery they manifested relative to the level predicted by the recovery function. Notably, their individuation relative to the mean recovery curve seemed to be set early in the recovery process and remained relatively stable at later time points. This additional modulation of individuation implies a second recovery process adding to the process represented by the mean recovery function.

Thus we propose that recovery of strength and individuation relies on partially separable systems. One system contributes all of strength and some degree of individuation. The isolated contribution of this system would determine the lower bound of the data points in the strength-individuation plot (dashed line in Fig. 5): a patient regains some strength and a limited amount of control. However, the amount of individuation is limited and does not increase above a certain level. This would explain both the strong correlation between strength and individuation for the severely impaired patients and the fact that no patient occupied the *bottom right* corner of strength-individuation space, i.e., no patients had good strength but minimal control. This recovery principle may be applicable to effectors beyond the hand: we have recently demonstrated a similar dissociation in strength and control for arm recovery in a subset of the same cohort of patients (Cortes et al. 2017).

The second system would then add additional individuation (control capacity) to the first system (vertical arrows in Fig. 5). Patients with a strong contribution from this second system may gain full recovery of individuation; patients with no or only partial contribution from the second system may recover strength completely, but not individuation. Importantly, the recovery of this second system also occurs early following stroke, after which a patient's relative position above or below the mean recovery function remains relatively fixed (Fig. 4D).

Lesion analysis adds support to the two-system model for recovery suggested by the behavioral data. A wealth of evidence in humans and nonhuman primates implicates the role of CST in finger control, especially the monosynaptic corticomotoneuronal (CM) connections originating from "new" M1 (Rathelot and Strick 2006, 2009). Notably, these connections do not generate high levels of force, but rather finely graded forces riding on top of larger forces (Maier et al. 1993). Consistent with this idea, lesions in the gray matter of the hand areas in M1 (the main origin of corticospinal projections), as well as the CST, correlated more with impaired individuation than with strength. In contrast, finger strength may rely on other neural pathways, including the RST, which can support strength and gross movements (Buford and Davidson 2004; Davidson and Buford 2004). Although the RST has been found to participate in some degree of finger control, its functional range is limited and biased toward flexor muscles (Baker 2011; Riddle et al. 2009).

Recovery after stroke is likely to result from the dynamic interplay between the CST and other descending pathways, particularly the RST. In this scenario, the correlation between strength and control at low levels of strength may represent the state of both the residual CST and of cortical projections to reticular nuclei in the brain stem. In contrast, recovery along the lower bound of the invariant function would represent the

contribution of the RST and other non-CST descending pathways, because strengthening of RST connections to motorneurons has been shown in monkeys with CST lesions (Zaaimi et al. 2012). Those patients with less damage to the CST would consistently ride above this function, reflecting better individuation ability. Although the origin of the corticoreticular inputs is more diffuse (Keizer and Kuypers 1989) and bilaterally organized (Buford and Davidson 2004; Sakai et al. 2009; Soteropoulos et al. 2012), many projections to the reticular formation arise from the "old" M1 (Catsman-Berrevoets and Kuypers 1976; Jones and Wise 1977). Our CST and hand M1 lesion ROIs, despite our best efforts, certainly will have been contaminated to some degree by non-CST fibers, including the corticoreticular tract and other corticofugal fibers synapsing in the brain stem. These additional descending pathways could in part explain the lower but nevertheless significant correlation with strength.

In summary, we show with a novel behavioral paradigm that recovery of hand function reflects the interplay between two independent systems. One contributes strength and some degree of fine motor control. The second system then provides additional fine motor control.

DISCLOSURES

No conflicts of interest, financial or otherwise, are declared by the authors.

AUTHOR CONTRIBUTIONS

J.X., J.W.K., and J.D. conceived and designed research; J.X., B.H., M.B., M.W., M.D.H., J.C.C., N.K., and T.K. performed experiments; J.X., N.E., A.V.F., and J.D. analyzed data; J.X., N.E., J.W.K., and J.D. interpreted results of experiments; J.X. prepared figures; J.X. drafted manuscript; J.X., N.E., J.W.K., and J.D. edited and revised manuscript; J.X., N.E., B.H., M.B., M.W., A.V.F., M.D.H., J.C.C., N.K., P.A.C., T.K., A.R.L., J.W.K., and J.D. approved final version of manuscript.

REFERENCES

Baker SN. The primate reticulospinal tract, hand function and functional recovery. *J Physiol* 589: 5603–5612, 2011. doi:10.1113/jphysiol.2011.215160.

Bates D, Mächler M, Bolker B, Walker S. Fitting linear mixed-effects models using lme4. *J Stat Softw* 67: 1–48, 2015. doi:10.18637/jss.v067.i01.

Brainard DH. The Psychophysics Toolbox. *Spat Vis* 10: 433–436, 1997. doi:10.1163/156856897X00357.

Buford JA, Davidson AG. Movement-related and preparatory activity in the reticulospinal system of the monkey. *Exp Brain Res* 159: 284–300, 2004. doi:10.1007/s00221-004-1956-4.

Catsman-Berrevoets CE, Kuypers HG. Cells of origin of cortical projections to dorsal column nuclei, spinal cord and bulbar medial reticular formation in the rhesus monkey. *Neurosci Lett* 3: 245–252, 1976. doi:10.1016/0304-3940(76)90050-1.

Ceritoglu C, Oishi K, Li X, Chou M-C, Younes L, Albert M, Lyketsos C, van Zijl PCM, Miller MI, Mori S. Multi-contrast large deformation diffeomorphic metric mapping for diffusion tensor imaging. *Neuroimage* 47: 618–627, 2009. doi:10.1016/j.neuroimage.2009.04.057.

Colebatch JG, Gandevia SC. The distribution of muscular weakness in upper motor neuron lesions affecting the arm. *Brain* 112: 749–763, 1989. doi:10.1093/brain/112.3.749.

Connolly K, Elliott J. The evolution and ontogeny of hand function. In: *Ethological Studies of Child Behaviour*, edited by Jones NB. Oxford: Cambridge University Press, 1972, p. x, 749–400.

Cortes JC, Goldsmith J, Harran MD, Xu J, Kim N, Schambra HM, Luft AR, Celnik P, Krakauer JW, Kitago T. A short and distinct time window for recovery of arm motor control early after stroke revealed with a global measure of trajectory kinematics. *Neurorehabil Neural Repair* 31: 552–560, 2017. doi:10.1177/1545968317697034.

Dale AM, Fischl B, Sereno MI. Cortical surface-based analysis. I. Segmentation and surface reconstruction. *Neuroimage* 9: 179–194, 1999. doi:10.1006/nimg.1998.0395.

Davidson AG, Buford JA. Motor outputs from the primate reticular formation to shoulder muscles as revealed by stimulus-triggered averaging. *J Neurophysiol* 92: 83–95, 2004. doi:10.1152/jn.00083.2003.

Duncan PW, Goldstein LB, Matchar D, Divine GW, Feussner J. Measurement of motor recovery after stroke. Outcome assessment and sample size requirements. *Stroke* 23: 1084–1089, 1992. doi:10.1161/01.STR.23.8.1084.

Fischl B, Rajendran N, Busa E, Augustinack J, Hinds O, Yeo BT, Mohlberg H, Amunts K, Zilles K. Cortical folding patterns and predicting cytoarchitecture. *Cereb Cortex* 18: 1973–1980, 2008. doi:10.1093/cercor/bhm225.

Fisher RA. On the "probable error" of a coefficient of correlation deduced from a small sample. *Metron* 1: 3–32, 1921.

Fugl-Meyer AR, Jääskö L, Leyman I, Olsson S, Steglind S. The post-stroke hemiplegic patient. 1. A method for evaluation of physical performance. *Scand J Rehabil Med* 7: 13–31, 1975.

Guttman L. A basis for analyzing test-retest reliability. *Psychometrika* 10: 255–282, 1945. doi:10.1007/BF02288892.

Heller A, Wade DT, Wood VA, Sunderland A, Hewer RL, Ward E. Arm function after stroke: measurement and recovery over the first three months. *J Neurol Neurosurg Psychiatry* 50: 714–719, 1987. doi:10.1136/jnnp.50.6.714.

Holland PW, Welsch RE. Robust regression using iteratively reweighted least-squares. *Commun Stat Theory Methods* 6: 813–827, 1977. doi:10.1080/03610927708827533.

Jones EG, Wise SP. Size, laminar and columnar distribution of efferent cells in the sensory-motor cortex of monkeys. *J Comp Neurol* 175: 391–437, 1977. doi:10.1002/cne.901750403.

Jørgensen HS, Nakayama H, Raaschou HO, Vive-Larsen J, Støier M, Olsen TS. Outcome and time course of recovery in stroke. Part II: Time course of recovery. The Copenhagen Stroke Study. *Arch Phys Med Rehabil* 76: 406–412, 1995. doi:10.1016/S0003-9993(95)80568-0.

Kamper DG, Harvey RL, Suresh S, Rymer WZ. Relative contributions of neural mechanisms versus muscle mechanics in promoting finger extension deficits following stroke. *Muscle Nerve* 28: 309–318, 2003. doi:10.1002/mus.10443.

Kamper DG, Rymer WZ. Impairment of voluntary control of finger motion following stroke: role of inappropriate muscle coactivation. *Muscle Nerve* 24: 673–681, 2001. doi:10.1002/mus.1054.

Keizer K, Kuypers HG. Distribution of corticospinal neurons with collaterals to the lower brain stem reticular formation in monkey (*Macaca fascicularis*). *Exp Brain Res* 74: 311–318, 1989. doi:10.1007/BF00248864.

Krakauer JW, Carmichael ST, Corbett D, Wittenberg GF. Getting neurorehabilitation right: what can be learned from animal models? *Neurorehabil Neural Repair* 26: 923–931, 2012. doi:10.1177/1545968312440745.

Laird NM, Ware JH. Random-effects models for longitudinal data. *Biometrics* 38: 963–974, 1982. doi:10.2307/2529876.

Lang CE, Schieber MH. Differential impairment of individuated finger movements in humans after damage to the motor cortex or the corticospinal tract. *J Neurophysiol* 90: 1160–1170, 2003. doi:10.1152/jn.00130.2003.

Lang CE, Schieber MH. Reduced muscle selectivity during individuated finger movements in humans after damage to the motor cortex or corticospinal tract. *J Neurophysiol* 91: 1722–1733, 2004. doi:10.1152/jn.00805.2003.

Lawrence DG, Kuypers HG. The functional organization of the motor system in the monkey. II. The effects of lesions of the descending brain-stem pathways. *Brain* 91: 15–36, 1968a. doi:10.1093/brain/91.1.15.

Lawrence DG, Kuypers HG. The functional organization of the motor system in the monkey. I. The effects of bilateral pyramidal lesions. *Brain* 91: 1–14, 1968b. doi:10.1093/brain/91.1.1.

Leigh R, Oishi K, Hsu J, Lindquist M, Gottesman RF, Jarso S, Crainiceanu C, Mori S, Hillis AE. Acute lesions that impair affective empathy. *Brain* 136: 2539–2549, 2013. doi:10.1093/brain/awt177.

Li S, Latash ML, Yue GH, Siemionow V, Sahgal V. The effects of stroke and age on finger interaction in multi-finger force production tasks. *Clin Neurophysiol* 114: 1646–1655, 2003. doi:10.1016/S1388-2457(03)00164-0.

Li ZM, Latash ML, Zatsiorsky VM. Force sharing among fingers as a model of the redundancy problem. *Exp Brain Res* 119: 276–286, 1998. doi:10.1007/s002210050343.

Lyle RC. A performance test for assessment of upper limb function in physical rehabilitation treatment and research. *Int J Rehabil Res* 4: 483–492, 1981. doi:10.1097/00004356-198112000-00001.

Maier MA, Bennett KM, Hepp-Reymond MC, Lemon RN. Contribution of the monkey corticomotoneuronal system to the control of force in precision grip. *J Neurophysiol* 69: 772–785, 1993.

Mori S, Oishi K, Jiang H, Jiang L, Li X, Akhter K, Hua K, Faria AV, Mahmood A, Woods R, Toga AW, Pike GB, Neto PR, Evans A, Zhang J, Huang H, Miller MI, van Zijl P, Mazziotta J. Stereotaxic white matter atlas based on diffusion tensor imaging in an ICBM template. *Neuroimage* 40: 570–582, 2008. doi:10.1016/j.neuroimage.2007.12.035.

Mori S, Wakana S, Nagae-Poetscher LM, Van Zijl PC. *MRI Atlas of Human White Matter* (1st ed.). Amsterdam: Elsevier Science, 2005, p. 1384–1385.

Napier JR. The prehensile movements of the human hand. *J Bone Joint Surg Br* 38-B: 902–913, 1956.

Noskin O, Krakauer JW, Lazar RM, Festa JR, Handy C, O'Brien KA, Marshall RS. Ipsilateral motor dysfunction from unilateral stroke: implications for the functional neuroanatomy of hemiparesis. *J Neurol Neurosurg Psychiatry* 79: 401–406, 2008. doi:10.1136/jnnp.2007.118463.

Oishi K, Faria AV, van Zijl PC, Mori S. *MRI Atlas of Human White Matter* (2nd ed.). Waltham, MA: Academic, 2010.

Oishi K, Zilles K, Amunts K, Faria A, Jiang H, Li X, Akhter K, Hua K, Woods R, Toga AW, Pike GB, Rosa-Neto P, Evans A, Zhang J, Huang H, Miller MI, van Zijl PCM, Mazziotta J, Mori S. Human brain white matter atlas: identification and assignment of common anatomical structures in superficial white matter. *Neuroimage* 43: 447–457, 2008. doi:10.1016/j.neuroimage.2008.07.009.

Oldfield RC. The assessment and analysis of handedness: the Edinburgh inventory. *Neuropsychologia* 9: 97–113, 1971. doi:10.1016/0028-3932(71)90067-4.

Picard RR, Cook RD. Cross-validation of regression models. *J Am Stat Assoc* 79: 575–583, 1984. doi:10.1080/01621459.1984.10478083.

R Core Team. *R: A Language and Environment for Statistical Computing.* Vienna: R Foundation for Statistical Computing, 2014.

Rathelot JA, Strick PL. Muscle representation in the macaque motor cortex: an anatomical perspective. *Proc Natl Acad Sci USA* 103: 8257–8262, 2006. doi:10.1073/pnas.0602933103.

Rathelot JA, Strick PL. Subdivisions of primary motor cortex based on cortico-motoneuronal cells. *Proc Natl Acad Sci USA* 106: 918–923, 2009. doi:10.1073/pnas.0808362106.

Reinkensmeyer DJ, Lum PS, Lehman SL. Human control of a simple two-hand grasp. *Biol Cybern* 67: 553–564, 1992. doi:10.1007/BF00198762.

Riddle CN, Edgley SA, Baker SN. Direct and indirect connections with upper limb motoneurons from the primate reticulospinal tract. *J Neurosci* 29: 4993–4999, 2009. doi:10.1523/JNEUROSCI.3720-08.2009.

Sakai ST, Davidson AG, Buford JA. Reticulospinal neurons in the pontomedullary reticular formation of the monkey (*Macaca fascicularis*). *Neuroscience* 163: 1158–1170, 2009. doi:10.1016/j.neuroscience.2009.07.036.

Schieber MH. Individuated finger movements of rhesus monkeys: a means of quantifying the independence of the digits. *J Neurophysiol* 65: 1381–1391, 1991.

Soteropoulos DS, Williams ER, Baker SN. Cells in the monkey pontomedullary reticular formation modulate their activity with slow finger movements. *J Physiol* 590: 4011–4027, 2012. doi:10.1113/jphysiol.2011.225169.

Sukal TM, Ellis MD, Dewald JPA. Shoulder abduction-induced reductions in reaching work area following hemiparetic stroke: neuroscientific implications. *Exp Brain Res* 183: 215–223, 2007. doi:10.1007/s00221-007-1029-6.

Sunderland A, Tinson D, Bradley L, Hewer RL. Arm function after stroke. An evaluation of grip strength as a measure of recovery and a prognostic indicator. *J Neurol Neurosurg Psychiatry* 52: 1267–1272, 1989. doi:10.1136/jnnp.52.11.1267.

Wakana S, Caprihan A, Panzenboeck MM, Fallon JH, Perry M, Gollub RL, Hua K, Zhang J, Jiang H, Dubey P, Blitz A, van Zijl P, Mori S. Reproducibility of quantitative tractography methods applied to cerebral white matter. *Neuroimage* 36: 630–644, 2007. doi:10.1016/j.neuroimage.2007.02.049.

Witham CL, Fisher KM, Edgley SA, Baker SN. Corticospinal inputs to primate motoneurons innervating the forelimb from two divisions of primary motor cortex and area 3a. *J Neurosci* 36: 2605–2616, 2016. doi:10.1523/JNEUROSCI.4055-15.2016.

World Health Organization. *Internationat Classification of Functioning, Disability and Health: ICF.* Geneva, Switzerland: World Health Organization, 2001.

Xu J, Haith AM, Krakauer JW. Motor control of the hand before and after stroke. In: *Clinical Systems Neuroscience*, edited by Kansaku K, Cohen LG, and Birbaumer N. Tokyo: Springer, 2015, p. 271–289. doi:10.1007/978-4-431-55037-2_14.

Yousry TA, Schmid UD, Alkadhi H, Schmidt D, Peraud A, Buettner A, Winkler P. Localization of the motor hand area to a knob on the precentral gyrus. A new landmark. *Brain* 120: 141–157, 1997. doi:10.1093/brain/120.1.141.

Zaaimi B, Edgley SA, Soteropoulos DS, Baker SN. Changes in descending motor pathway connectivity after corticospinal tract lesion in macaque monkey. *Brain* 135: 2277–2289, 2012. doi:10.1093/brain/aws115.

Zatsiorsky VM, Li ZM, Latash ML. Enslaving effects in multi-finger force production. *Exp Brain Res* 131: 187–195, 2000. doi:10.1007/s002219900261.

Zhang W, Olivi A, Hertig SJ, van Zijl P, Mori S. Automated fiber tracking of human brain white matter using diffusion tensor imaging. *Neuroimage* 42: 771–777, 2008. doi:10.1016/j.neuroimage.2008.04.241.

Zhang Y, Zhang J, Oishi K, Faria AV, Jiang H, Li X, Akhter K, Rosa-Neto P, Pike GB, Evans A, Toga AW, Woods R, Mazziotta JC, Miller MI, van Zijl PC, Mori S. Atlas-guided tract reconstruction for automated and comprehensive examination of the white matter anatomy. *Neuroimage* 52: 1289–1301, 2010. doi:10.1016/j.neuroimage.2010.05.049.